Thermochimica Acta 483 (2009) 73–77

Contents lists available at ScienceDirect

Thermochimica Acta

journal homepage: www.elsevier.com/locate/tca

Short communication

Thermal energy storage behavior of Al_2O_3–H_2O nanofluids

Shuying Wu*, Dongsheng Zhu, Xinfang Li, Hua Li, Junxi Lei

Key Lab of Enhanced Heat Transfer and Energy Conservation, The Ministry of Education, School of Chemistry and Chemical Engineering, South China University of Technology, Guangzhou 510641, PR China

ARTICLE INFO

Article history:
Received 29 April 2008
Received in revised form 9 October 2008
Accepted 18 November 2008
Available online 27 November 2008

Keywords:
Al_2O_3–H_2O nanofluids
Supercooling degree
Freezing time
Thermal energy storage

ABSTRACT

This study aims to evaluate the potential of Al_2O_3–H_2O nanofluids as a new phase change material for the thermal energy storage of cooling systems. Different mass fractions of nanofluids were prepared through adding Al_2O_3 nanoparticles and sodium dodecylbenzenesulfonate into water solution at 1 h of ultrasonic vibration. Measurement of particle size and zeta potential of nanofluids shows that Al_2O_3 nanoparticles have good dispersion in water, but Al_2O_3–H_2O nanofluids with high mass fraction will make nanoparticles easier to aggregate. The thermal response test shows the addition of Al_2O_3 nanoparticles remarkably decreases the supercooling degree of water, advances the beginning freezing time and reduces the total freezing time. In order to visually observe the freezing process, an infrared imaging experimental system was built. The photographs suggest that the freezing rate of nanofluids is enhanced. Only adding 0.2 wt% Al_2O_3 nanoparticles, the total freezing time of Al_2O_3–H_2O nanofluids can be reduced by 20.5%.

1. Introduction

The imbalance of electrical demand in summer causes a big problem in many countries and stabilizing power demand is required [1,2]. One solution of shifting peak demand in the early afternoon to the night is achieved by running refrigerators driven by night-time power and storing cold energy during the night [3]. However, from the point of view of heat loss and refrigerator performance, energy efficiencies of present storage systems are not so good, such as ice and gas hydrate storage systems [4,5]. The problems of supercooling, poor thermal conductivity and large investment cost exist. Therefore, there have been strong demands for more efficient energy storage materials in many industries. The novel concept of 'nanofluids' – heat transfer fluids containing suspensions of nanoparticles – has been proposed as a means of meeting these challenges [6,7]. The industrial groups that would benefit from such improved heat transfer fluids are quite varied, including transportation, electronics cooling, nuclear systems cooling, biomedicine, and food of many types [8–10].

Nanofluids are solid–liquid composite materials consisting of solid nanoparticles or nanofibers with sizes typically of 1–100 nm suspended in liquid. It has been shown that nanoparticles with higher thermal conductivity than their surrounding liquid can increase the effective thermal conductivity of suspension. For example, a small amount (<1% volume fraction) of Cu nanoparticles or carbon nanotubes dispersed in water or oil was reported to increase the inherently poor thermal conductivity of the liquid by 74% and 150% [11,12]. Furthermore, the 300% enhancement of thermal conductivity observed by Philip was achieved by a Fe_3O_4 nanoparticle loading of 6.3 vol.% [13]. Compared with millimeter – or micrometer – sized particle suspensions, nanofluids possess better long-term stability, much higher surface area and rheological properties. However, recent efforts have mainly been focused on the thermal conductivity [14–16] and viscosity [17,18] of water or oil-based with Al_2O_3 and very few reports of the thermal behavior of H_2O-based nanofluids have been found, expect for the latest research on the specific heat capacity of Al_2O_3–H_2O nanofluids by Zhoua and Ni [19].

The main purpose of this study is to prepare and evaluate the thermal properties of Al_2O_3–H_2O nanofluids.

Therefore, if the thermal properties of Al_2O_3–H_2O nanofluids are better than that of H_2O, we can use them as a thermal energy storage material in cooling systems and the imbalance of electrical demand in summer may be alleviated. The ceramic nanoparticle was chosen for cool storage because it had an electric insulation property. The stability analysis of Al_2O_3–H_2O nanofluids was estimated with a Malvern ZS NanoS analyzer. A thermal response test was performed to evaluate the phase change characteristics of Al_2O_3–H_2O nanofluids and H_2O. To investigate the freezing rate of Al_2O_3–H_2O nanofluids, the infrared imaging instrument was employed. At the same time, we compared the experimental results with those of other groups.

* Corresponding author. Tel.: +86 20 8711 4140.
E-mail address: wushuying5876@126.com (S. Wu).

0040-6031/$ – see front matter © 2008 Elsevier B.V. All rights reserved.
doi:10.1016/j.tca.2008.11.006

2. Experimental

2.1. Materials

Commercial spherical-shape Al_2O_3 powders (Alfa Aesar, Ward Hill, MA, USA) with Al_2O_3 content >99.98% and an average diameter of 20 nm were used. An anionic surfactant, sodium dodecylbenzenesulfonate (referred as SDBS) in chemical grade, was purchased from Guangzhou Chemical Reagent Factory (China). The double-distilled water was used as a base fluid. All chemicals were used as received without any further purification.

2.2. Preparation method

Two-step method was selected to prepare the nanofluids. In order to minimize particle aggregation and improve dispersion behavior, two effective methods were carried out in this study: (1) using SDBS as the dispersant. In previous research, we have proved that the most suitable concentration ratio of nanoparticles to SDBS dispersant is 1:1 (w/w) [20]. (2) Using ultrasonic vibration. Ultrasonication is an accepted technique for dispersing the highly entangled or aggregated nanoparticle samples [21–23], but longer time of high-energy sonication can introduce defects.

2.3. Instrumentation

The ultrasonic cleanser (KQ2200DE, Kunshan of Jiangsu Equipment Company, China) was used to disperse Al_2O_3 nanoparticles and SDBS into distilled water. Then the particle size and zeta potential of the nanofluids were measured by a Malvern ZS NanoS analyzer (Malvern Instrument Inc., London, UK). The measurement was run at $V = 10$ V, $T = 25\,^{\circ}$C with the switch time at $t = 50$ s. The transient hot-wire analysis instrument (Hotdisk AB Company, Sweden) was employed to measure the thermal conductivity of nanofluids. A 10-μm diameter nickel wire was chosen. Each experiment was repeated six times to calculate the mean value of the experimental data. The thermal conductivities with the deionized water are 0.5706 W/(m K) at 283 K, 0.6010 W/(m K) at 293 K and 0.6233 W/(m K) at 303 K. The base values are 0.5741 W/(m K), 0.5985 W/(m K) and 0.6171 W/(m K), respectively. So, the uncertainty on thermal conductivities is less than ±1.00%.

The thermal response test was performed on a low constant temperature trough (DC2006, Institute of Xinzhi Scientific Instrument, Ningbo, China). The temperatures inside test tubes were measured by 0.2 mm Ø sheathed T-type thermocouples. The test precision of thermocouples is ±0.2 °C. The temperature datalogger (Agient 34970A) was used to collect the values of temperatures and the time interval was 30 s. The temperature distribution of the sample surface was observed by an infrared imaging instrument (TH9100 MV/WV, NEC, Japan).

2.4. Experimental procedure

The experimental setup for the thermal response test is shown in Fig. 1. The glycol–water mixture was poured into the low constant temperature trough and worked as coolant. The volume ratio of glycol and water was 1:1. The nanofluids of 0.05 wt%, 0.1 wt%, 0.2 wt% and distilled water were transferred into four test tubes. These tubes were put into the low constant temperature trough. In the test, the temperature of glycol–water mixture was kept at −20 °C during the cooling period and at 15 °C during the heating period. The temperature change with time was recorded by the temperature datalogger. Because the diameter of test tubes was too small to be convenient to take photographs, four 150 ml beakers filled with 50 ml suspensions were put into the low constant temperature trough. At this time, the temperature of glycol–water mixture was kept at −15 °C. The time interval of taking photographs was 1 min. The advantages of this experimental system were quick, real-time and convenient.

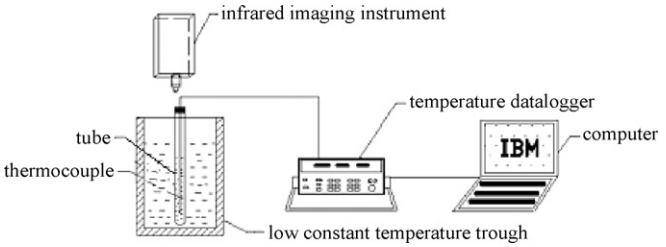

Fig. 1. Experimental setup for the thermal response test.

3. Results and discussions

3.1. Preparation and stability evaluation of nanofluids

In the study, Al_2O_3 nanoparticles (0.2 g) and a water solution (99.6 g) with SDBS dispersant (0.2 g) were directly mixed in a 150 ml beaker. The precision of electronic balance is ±0.0001 g. The suspension was transferred into an ultrasonic vibrator and sonicated for 1 h at a frequency of 40 kHz and an output power of 100 W at 25–30 °C. For the comparison, the suspension without SDBS dispersant was sonicated for 1 h in the same way. Fig. 2 illustrates the particle size distributions of Al_2O_3–H_2O nanofluids in the absence (a) and in the presence (b) of SDBS dispersant, which shows that there are obvious variations in the particle size characteristics between two samples. The particle size distributions of Al_2O_3–H_2O nanofluids without SDBS dispersant possess three peaks, which suggest that nanofluids without SDBS dispersant are poor dispersion and agglomerate resulting in non-uniform distribution. The average particle sizes obtained are (a) in the absence of SDBS dispersant: 433 nm and (b) in the presence of SDBS dispersant: 259 nm. Therefore, the stabilization of Al_2O_3–H_2O suspension with SDBS dispersant is better.

The stability of Al_2O_3 powder suspension in aqueous solution is closely related to its electrophoretic properties [24,25]. Meanwhile, the values of particle size can really reflect the dispersion of Al_2O_3 particles in water. So, the measurement of the particle size and zeta potential of nanofluids was performed. For the measurement of zeta potential, the maximum mass fraction of Al_2O_3 nanoparticles was 0.2 wt%, a higher content was not suitable. The results are shown in Fig. 3. It has been reported that the nanoparticle

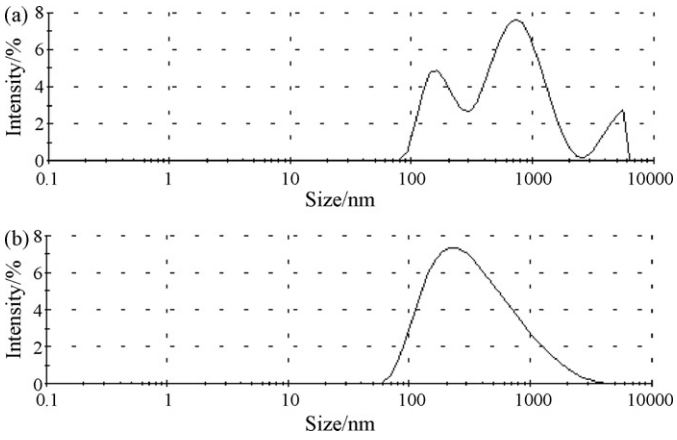

Fig. 2. Particle size distributions of Al_2O_3–H_2O suspensions in the absence (a) and in the presence (b) of SDBS dispersant. Mass fractions of Al_2O_3 and SDBS dispersant are both 0.2 wt%.

Table 1
Supercooling degree and freezing time for Al_2O_3 nanofluids and deionized water.

Mass fraction (%)	T_n (°C)	T_m (°C)	ΔT (°C)	$(\Delta T_f - \Delta T_{nf})/\Delta T_f$ (%)	Total freezing time (s)
0.0	−7.8	0.1	7.9		900
0.05	−4.0	1.1	5.1	35.4	840
0.1	−2.4	1.1	3.5	55.7	780
0.2	−1.3	1.0	2.3	70.9	690

Notes: T_n, supercooling temperature; T_m, phase change temperature; ΔT, supercooling degree, $\Delta T = T_m - T_n$; ΔT_f, the supercooling degree of water; ΔT_{nf}, the supercooling degree of nanofluids.

suspension becomes a stable dispersion with a high absolute value of zeta potential ($|\xi| > 30$ mV) [26]. In our work, all the absolute values of zeta potential are above 30 mV, which is a little higher than the results of Lee et al. [27], probably due to the stability effects of SDBS dispersant. When the concentration of nanofluids increases, it provides more collision chances of Al_2O_3 nanoparticles. Hence, the nanoparticles become easier to aggregate and the values of particle size become bigger. In this study, the absolute values of zeta potential and the values of particle size simultaneously indicate that the Al_2O_3–H_2O nanofluids have good stability and the following work can be gone on.

3.2. Thermal response test of the nanofluids

In order to investigate the effects of Al_2O_3 nanoparticles on the base fluid, a thermal response test was built. The typical temperature versus time curves of the nanofluids and water are shown in Fig. 4. Al_2O_3–H_2O nanofluids have remarkably lower supercooling degree than water, and the beginning nucleation time of nanofluids is ahead of H_2O. Moreover, the total freezing time is lower than that of H_2O. For other materials, a similar shape of curves was reported by Liu et al. [28] and Bílen et al. [29].

Along with the concentration increase of Al_2O_3–H_2O nanofluids, the supercooling degree decreases significantly. Only adding 0.05 wt% of Al_2O_3 nanoparticle, the supercooling degree can be reduced by 35.4%. The supercooling degree of 0.2 wt% Al_2O_3–H_2O nanofluid is 2.3 °C, which is much lower than that of water (7.9 °C), and the elevation rate is 70.9%. This result is in concordance with the studies of Liu [30], who investigated the thermal properties of $BaCl_2$–H_2O solution with TiO_2 nanoparticles. He concluded that the supercooling degree was reduced by 84.9% with suspending 1.13 vol.% nanoparticles in solution. The improvement of supercooling degree can be explained by the mechanism of heterogeneous nucleation. In the freezing process, Al_2O_3 nanoparticles act as a nucleating agent. The principle of similar structure and corresponding dimension is that the crystal face structure of nanoparticles and base fluid is more similar, the surface free energy ΔG_c will be less [30]. According to this principle, the size of Al_2O_3 nanoparticle is about 20 nm, which is close to water. Thus, ΔG_c between nanoparticles and water is little, and the wetting and contacting between them can be very well. The supercooling degree can be improved by the addition of nanoparticles.

Fig. 4 also shows the phase change of Al_2O_3–H_2O nanofluids starts at 1 °C, which is higher that H_2O. These results suggest that the phase change temperature is independent of the mass fraction of nanoparticles. The same experimental results were also found by Liu et al. [30] and Alvarado et al. [31]. The possible reason is the Al_2O_3 nanoparticle number mainly effect on the supercooling degree due to the heterogeneous nucleation mechanism. The experimental data of Montenegro and Landfester [32] show that the initiation of freezing temperature depends on particle size. Meanwhile, the beginning freezing time of 0.2 wt% sample is at 429 s and the total freezing process spends 690 s,which is much shorter than that of water (900 s). The specific values of phase change temperature, supercooling degree and freezing time are listed in Table 1.

After the freezing process, the release of sensible heat begins. It does not finish until the temperatures inside the test tubes equal to the setting temperature of the low constant temperature trough. In this process, the temperature change rates of nanofluids become slower than those of water. Then, the heating process follows subsequently and the ice begins to melt. As can be clearly seen from Fig. 4 that the cool discharge rate of the 0.2 wt% is the quickest in the four samples. For these samples, there is little difference between the melting point and the freezing point, which is an important element for a stable phase change material. Hence, the Al_2O_3–H_2O nanofluids have the potential application in cooling systems.

3.3. Freezing process of nanofluids

In order to vividly and visually observe the ice formation, an infrared imaging experimental system was built. The temperature-variation photographs of freezing process are shown in Fig. 5(a)–(f).

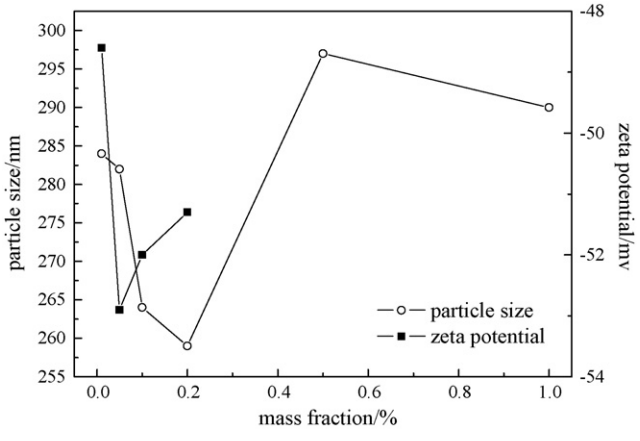

Fig. 3. Plot of particle size and zeta potential versus mass fraction for Al_2O_3–H_2O suspension.

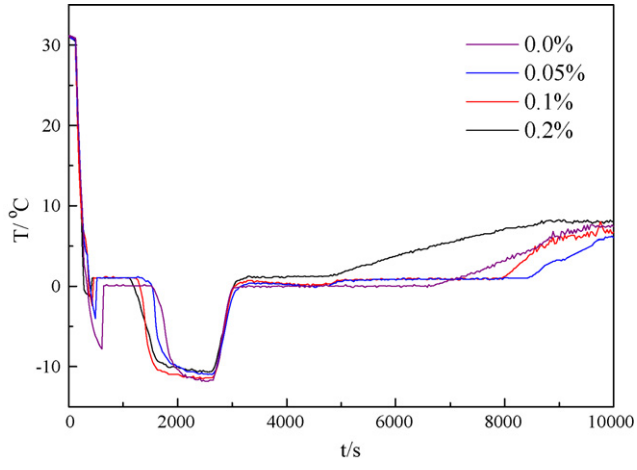

Fig. 4. Timewise variation of the Al_2O_3–H_2O nanofluid temperatures.

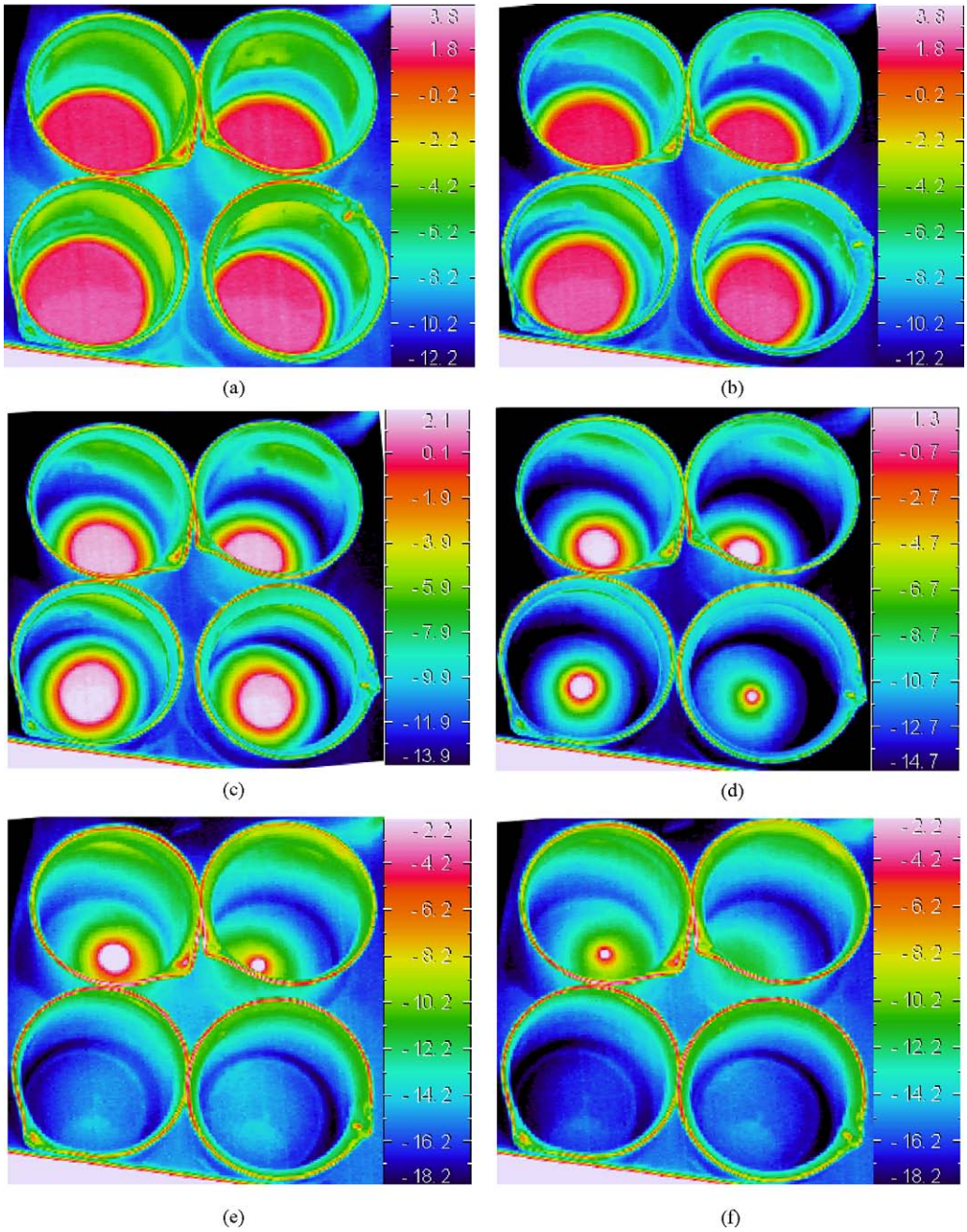

Fig. 5. The temperature profiles in the freezing process: (a) $t = 1$ min; (b) $t = 10$ min; (c) $t = 20$ min; (d) $t = 30$ min; (e) $t = 36$ min; (f) $t = 38$ min. The concentration of the top suspensions is 0.0 wt%, 0.05 wt%; the concentration of the bottom suspensions is 0.1 wt%, 0.2 wt%.

The photographs show that the ice grows from the breaker wall to the beaker center and forms a ringlike structure. As the test time increases further, the ring gets smaller and smaller. At last, it disappears and the whole freezing process finishes. These photographs also suggest that the concentration of nanofluids is higher, the freezing rate is quicker. At the beginning, the temperatures of four samples are all the same. Their temperature difference becomes obvious along with time. The whole freezing time of distilled water is 39 min, 0.05 wt% nanofluid 36 min, 0.1 wt% nanofluid 33 min, and 0.2 wt% nanofluid 31 min. It is evident that the freezing time is shorter when the concentration is higher. Only adding 0.2 wt% Al_2O_3 nanoparticles into water, the freezing time of can be saved by 20.5%. This phenomenon is in agreement with the study of Khodadadi and Hosseinizadeh [33], who investigated the Cu–H_2O nanofluids for thermal energy storage by computational simulation. However, it is not to say that the more nanoparticles are added, the time will be saved more. With the increasing of nanoparticles, other problems will be brought, dispersion stability, specific heat, viscosity, etc. So, it is recommended that care to taken when adding nanoparticles.

The behavior of saving time can be explained from the view of heat transfer, because the crystal growth mainly depends on heat transfer. At the process of freezing, large amount of heat will be discharged. If the heat cannot be released timely, the freezing process will be hindered. After adding the nanoparticles to the base fluid, the fluid has higher thermal conductivity. Therefore, the freezing speed of growth is able to be accelerated. Thermal conductivities of samples were measured by the transient hot-wire method. The values of 0.0 wt%, 0.05 wt%, 0.1 wt% and 0.2 wt% Al_2O_3–H_2O nanofluids are 0.6008 W/(m K), 0.6483 W/(m K), 0.6525 W/(m K)

and 0.6639 W/(m K) at 21 °C, respectively. There is a different extent increasing of thermal conductivity, which has been verified by many other groups [34,35]. So, the thermal conductivity improvement of H_2O confirms to the reduction of freezing times of nanofluids with respect to freezing time of H_2O.

4. Conclusions

In order to solve the imbalance of electrical demand in summer and save energy, using the thermal energy storage of phase change material is one of the effective ideas. The potential of Al_2O_3–H_2O nanofluids as a new phase change material was investigated in this study. Al_2O_3–H_2O nanofluids were prepared by a two-step method. The measurement of particle size and zeta potential suggests the Al_2O_3 nanofluids have good dispersion and stability, but high mass fraction of Al_2O_3–H_2O nanofluids is easier to aggregate. The advantages of nanofluids are shown as following: (i) the supercooling degree decreases strongly; (ii) the phase change time is ahead; (iii) the phase change temperature of nanofluids enhances; (iv) the total freezing time is reduced; (v) the thermal conductivity increases. The supercooling degree of 0.2 wt% Al_2O_3–H_2O nanofluid is reduced by 70.9% and the beginning time of freezing is ahead by 32.9%. The phase change temperatures of nanofluids enhance to 1 °C. The maximum enhancement of thermal conductivity is 10.5%. The results of the infrared imaging experiment suggest that nanoparticles could enhance the freezing rate of fluids. Only adding 0.2 wt% Al_2O_3 nanoparticles into water, the total freezing time can be saved by 20.5%. Thus, the application of nanofluids in cooling industry can improve the performance of refrigeration systems and save the running time for refrigeration systems [36]. Also, the aim to save energy can be achieved. However, the viscosity of nanoparticle–water suspensions increases in accordance with increasing particle concentration in the suspension. So, the particle mass fraction cannot be increase unlimitedly.

Acknowledgments

The authors would like to acknowledge the financial supports from the National Natural Science Foundation of China (Grant No. 20346001), Program for New Century Excellent Talents in University (Grant No. NCET–04–0826), Specialized Research Fund for the Doctoral Program of Higher Education (Grant No. 20050561017).

References

[1] K.J. Baker, R.M. Rylatt, Appl. Energy 85 (2008) 475–482.
[2] K.L. Zhou, J.A. Ferreira, S.W.H. de Haan, Int. J. Hydrogen Energy 33 (2008) 477–489.
[3] M. Yamaha, N. Nakahara, R. Chiba, Int. J. Energy Res. 32 (2008) 226–241.
[4] S.M. Hasnain, Energy Convers. Manage. 39 (1998) 1139–1153.
[5] Z.G. Sun, R.Z. Wang, R.S. Ma, et al., Int. J. Energy Res. 27 (2003) 747–756.
[6] S.U.S. Choi, ASME FED 231 (1995) 99.
[7] Y.H. Wang, J.K. Lee, C.H. Lee, et al., Thermochim. Acta 455 (2007) 70–74.
[8] S.C. Tzeng, C.W. Lin, K.D. Huang, Acta Mech. 179 (2005) 11–23.
[9] R. Chein, J. Chuang, Int. J. Therm. Sci. 46 (2007) 57–66.
[10] M.K. Chaudhury, Nature 423 (2003) 131–132.
[11] S. Jana, A.S. Khojin, W.H. Zhong, Thermochim. Acta 462 (2007) 45–55.
[12] S.U.S. Choi, Z.G. Zhang, W. Yu, et al., Appl. Phys. Lett. 79 (2001) 2252–2254.
[13] J. Philip, P.D. Shima, B. Raj, Appl. Phys. Lett. 91 (2007) 203108.
[14] M.P. Beck, T.F. Sun, A.S. Teja, Fluid Phase Equilibr. 260 (2007) 275–278.
[15] C.H. Li, G.P. Peterson, J. Appl. Phys. 99 (2006) 084314.
[16] D.H. Yoo, K.S. Hong, H.S. Yang, Thermochim. Acta 455 (2007) 66–69.
[17] C.T. Nguyen, F. Desgranges, N. Galanis, et al., Int. J. Therm. Sci. 47 (2008) 103–111.
[18] R. Prasher, D. Song, J.L. Wang, Appl. Phys. Lett. 89 (2006) 133108.
[19] S.Q. Zhoua, R. Ni, Appl. Phys. Lett. 92 (2008) 093123.
[20] D.S. Zhu, H. Li, X.J. Wang, et al., Acta Sci. Naturalium Universitatis Sunyatseni 46 (2007) 254–255.
[21] J. Liu, A.G. Rinzler, H.J. Dai, et al., Science 280 (1998) 1253–1256.
[22] M.J. O'Connell, S.M. Bachilo, C.B. Huffman, et al., Science 297 (2002) 593–596.
[23] X.F. Li, D.S. Zhu, X.J. Wang, J. Colloids Interf. Sci. 310 (2007) 456–463.
[24] H. Karimian, A.A. Babaluo, J. Eur. Ceram. Soc. 27 (2007) 19–25.
[25] F. Aloulou, S. Boufia, D. Beneventi, J. Colloids Interf. Sci. 280 (2004) 350–358.
[26] R.H. Muüller, Zetapotential und Partikelladung in der Laborpraxis, first ed., Wissenschaftliche Verlagsgesellschaft, Stuttgart, 1996.
[27] J.H. Lee, K.S. Hwang, S.P. Jang, et al., Int. J. Heat Mass Trans. 51 (2008) 2651–2656.
[28] Y.D. Liu, M.W. Tong, Q.B. He, Mater. Rev. 19 (2005) 206–208.
[29] K. Bílen, F. Takgil, K. Kaygusuz, Energy Sources: Part A 30 (2008) 775–787.
[30] Y.D. Liu, Study on Preparation and Thermal Properties of Phase Change Nanocomposites for Cool Storage, Chongqing University, China, 2005.
[31] J.L. Alvarado, C. Marsh, C. Sohn, et al., J. Therm. Anal. Calorim. 36 (2006) 505–509.
[32] R. Montenegro, K. Landfester, Langmuir 19 (2003) 5996–6003.
[33] J.M. Khodadadi, S.F. Hosseinizadeh, Int. Commun. Heat Mass Trans. 34 (2007) 534–543.
[34] X.F. Li, D.S. Zhu, X.J. Wang, et al., Thermochim. Acta 469 (2008) 98–103.
[35] D. Wen, Y. Ding, Int. J. Heat Fluid Flow 26 (2005) 855–864.
[36] S.K. Das, Heat Trans. Eng. 27 (2006) 1–2.